

SIMULATIONS OF ICE CRYSTAL OPTICAL PROPERTIES AND CLOUD TOP RADIATIVE STRUCTURE OF DEEP CONVECTIVE STORMS IN THE MSG SEVIRI VIS AND IR CHANNELS

S. Melani¹, E. Cattani¹, V. Levizzani^{1*}, M. Cervino¹, F. Torricella¹,

T. Rother², M. Hess³, K. Schmidt²

¹ISAO-CNR, via Gobetti 101, I-40129 Bologna, Italy

²DLR, German Remote Sensing Data Center (DFD), Algorithms and Processors (AP),
Kalkhorstweg 53, D-17235 Neustrelitz, Germany

³DLR, German Remote Sensing Data Center (DFD), D-82234 Weßling, Germany

ABSTRACT

METEOSAT Second Generation (MSG) Spinning Enhanced Visible and Infrared Imager (SEVIRI) channels in the visible (VIS), near infrared (NIR) and thermal infrared (IR) open up new possibilities for cloud top structure studies from the microphysical, radiative and dynamical perspectives. Studies such as those of Levizzani and Setvák (1996) have indicated the existence of unexpected features on top of deep convection that could only be detected using satellite sensors: plumes of small ice crystals, rotational features and wave patterns. Several of these features are yet to be explained in their overall complexity since cloud dynamics and microphysics are involved at the same time. Deep convection is also being reconsidered as a very powerful engine for troposphere-to-stratosphere water vapor exchanges. Simulations of the optical properties of randomly oriented ice crystal particles on top of deep convective clouds are presented. Computations are based on a combined Mie and Huygens theory assuming columnar shapes of hexagonal section. Several ice crystal size ranges in the 2 to 20 μm interval were considered thereby producing different values of single scattering albedo, asymmetry factor and extinction coefficient. Real ice crystal size distributions at convective cloud top are simulated. Radiances at the top of deep convective storms are calculated for the following channels of the MSG SEVIRI: 0.8, 1.6, 3.9, 10.8 and 12 μm . Midlatitude cirrus anvils over deep convection are simulated to determine the SEVIRI channel sensitivity to changes in their radiative properties using the model STREAMER. Sensitivity is derived performing several tests varying the ice crystal size and the optical depth. Results are to be considered as a first tool to explore cloud top properties in conditions where *in situ* measurements are very much critical and very scarce data are available in the literature.

* Visiting Scientist at EUMETSAT, Darmstadt, Germany

1. INTRODUCTION

Peculiar cirrus features were found on top of several deep convective storms. Levizzani and Setvák (1996) identified them as “plumes” of small ice crystals because of their shape like a plume or a fan emanating from a relatively small spot. Their presence was detected by analyzing multispectral, high-resolution imagery from the Advanced Very High Resolution Radiometer (AVHRR) (see also Setvák and Doswell, 1991). They produce a significant increase of the AVHRR channel 3 (centered at $3.7 \mu\text{m}$) cloud-top reflectivity (Fig.1), which implies they are composed of ice crystals whose size is about $3\text{-}4 \mu\text{m}$. Moreover plumes constitute an independent upper-level structure separated from the surrounding cirrus anvil.

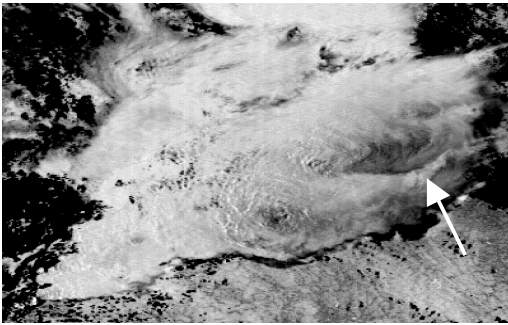


Figure 1. AVHRR NOAA-9 channel 3 ($3.7 \mu\text{m}$) cloud-top reflectivity image of a multicell storm over central Slovakia and southern Poland, 6 July 1988 1348 UTC. The darker shades correspond to higher reflectivity values. A plume feature can be seen on the right side of the image (see arrow) (from Levizzani and Setvák, 1996, courtesy of Amer. Meteor. Soc.).

This work represents a first approach to the characterization of these features in terms of particle size and optical depth using the MSG SEVIRI channels in the VIS, NIR and IR. The radiometer is very suitable for cloud top microphysical studies given its spectral channels (12 instead of 3 of the actual METEOSAT), spatial resolution of $3 \times 3 \text{ km}^2$, and the improved repeat cycle of 15 minutes. This will allow for a plume characterization by following their evolution without the limitations of an insufficient number of available passages on a single scene typical of the polar orbiters.

The radiative response of a midlatitude deep convective cloud was simulated in the SEVIRI channels centered at the wavelengths $0.8, 1.6, 3.9, 10.8, 12.0 \mu\text{m}$. The radiative transfer model STREAMER was used because of its flexibility in specifying the cloud structure. Simulations were carried out taking into account the spectral resolution of the instrument. A sensitivity analysis of the SEVIRI channels to the ice crystal size and optical depth of the cirrus layer on top of the deep convective cloud is performed in order to evaluate the radiative response of small ice crystals with respect to that of larger ice particles that normally compose a cirrus anvil.

A data set of optical properties (extinction coefficient β_{ext} , single-scattering albedo ω_0 , asymmetry parameter g) for small ice particles was given in input to simulate the cirrus layer on top of the deep convection. The data set was computed for hexagonal cylinders randomly oriented in space using a combined Mie and Huygens theory.

2. DATA SET OF THE OPTICAL PROPERTIES

Because of the limitations of STREAMER on the parameterization of the optical properties of ice clouds in the shortwave range in presence of small size particles ($< 15 \mu\text{m}$), a data set of optical properties ($\beta_{\text{ext}}, \omega_0, g$) was computed and input into the radiative transfer model. For each of the aforementioned SEVIRI channels $\beta_{\text{ext}}, \omega_0, g$ are calculated for hexagonal cylinders randomly oriented using a method based on a combined Mie and Huygens theory.

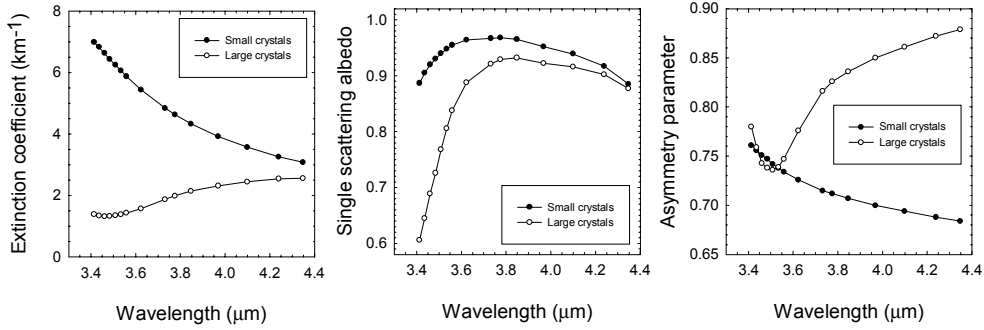


Figure 2. The ice crystal optical properties at 3.9 μm . The curves refer to two different length ranges of ice crystals: “small” crystals, [2, 6] μm , and “large” crystals, [6, 20] μm .

According to this method the exact solution for the corresponding infinitely long cylinder, obtained within the framework of the discretized Mie formalism and the generalisation of the method of separation of variables, is inserted into Huygens’ principle. The surface integration is confined to a finite cylinder length neglecting the contributions of the top and bottom faces. In this way an approximate solution for the corresponding finite cylinder is obtained (Havemann *et al.*, 1998; Rother, 1998; Rother, 1999; Rother and Schmidt, 1997; Rother *et al.*, 1997). The computations were performed for two length ranges of the ice particles, [2, 6] μm and [6, 20] μm , hereafter referred to as “small” and “large” crystals, respectively. In Fig.2 the optical properties for small and large ice crystals in the SEVIRI 3.9 μm channel are shown. There is a pronounced dependence of the single-scattering properties on the crystal size at these wavelengths, in particular the influence of the smaller crystals is strong. The higher values of β_{ext} and ω_0 of small crystals cause the incident radiation to be almost scattered in the first cloud layers, prevalently in the forward direction ($g \cong 0.79$). On the other hand, the larger crystals exhibit more absorption and lower extinction coefficient values, providing less contribution to the total signal.

3. THE RADIATIVE TRANSFER MODEL AND THE SIMULATIONS

The radiative transfer model used to simulate the SEVIRI measurements is STREAMER (Key, 1998; Key and Schweiger, 1998), a medium spectral resolution model based on the plane-parallel theory and the discrete ordinate solver DISORT (Stamnes *et al.*, 1988). It computes radiances and fluxes in the 0.28-500 μm range, covered by 129 variable-width bands. Its flexible interface for the specification of cloud and surface properties provides an effective tool for the present sensitivity analysis. The spectral response functions of SEVIRI channels are simulated by feeding STREAMER with the appropriate coefficients for weighting the spectral bands of the model, which are covered by the response functions. The absorption of atmospheric gases (H_2O , O_2 , CO_2 , O_3) is taken into account. The vertical profiles of pressure, temperature, water vapor and ozone are introduced using an appropriate number of vertically homogeneous plane-parallel layers. Finally, the radiative simulations were carried out assuming an aerosol-free atmosphere. The relevant inputs for the simulations are summarized in Table 1.

Input parameters	Selected Value(s)
Atmospheric profile	Midlatitude-summer
Wavelength λ	0.8, 1.6, 3.9, 10.8, 12 μm
Solar zenith angle θ_0	45°
Observer zenith angle θ	30°
Relative azimuth angle Φ	130°
Surface emissivity ϵ	0.96
Surface temperature T_s	294 K

Table 1. *Input parameters for the radiative transfer computations.*

The simulated cloud structure represents a deep convective cloud in its typical final growth phase, when a cirrus layer develops on its top (Fig. 3). It is a rather simplified cloud structure consisting of a cumulonimbus tower, with a water droplet cloud layer underlying an ice cloud layer, and a cirrus layer on top. The water cloud layer has an optical depth at 0.6 μm $\tau_{0.6}=40$ and a top height of 5 km, and the overlapping ice layer has the same optical depth and a top height of 9 km. The liquid and ice water contents (LWC and IWC) of the cumulonimbus were set to 0.3 and 0.5 g m^{-3} , respectively, and the water droplets and the ice crystals have an effective radius of 20 μm and 130 μm , respectively. The cirrus layer has an optical thickness varying from $\tau_{0.6}=0.1$ to 5 with $\Delta\tau_{0.6}=0.5$ and an IWC of 0.005 g m^{-3} . As previously described, the simulations were performed for small and large crystals.

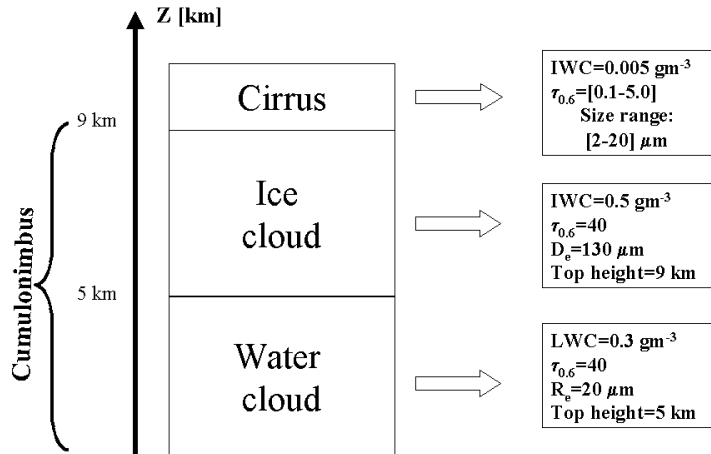


Figure 3. *Scheme of the simulated deep convective cloud. The characteristics of each layer composing the cloud structure are also reported in the figure.*

4. RESULTS

The sensitivity analysis of the SEVIRI channels was done computing the reflectances at 0.8, 1.6, 3.9 μm and the brightness temperatures at 10.8 and 12 μm . The thermal emission component was removed from the simulated radiances at 3.9 μm trying to simulate the response in reflectivity of cloud top small ice crystals.

In Fig. 4 the reflectance values at 1.6 μm are plotted as a function of the reflectance values at 0.8 μm . Note that reflectances at 0.8 μm are nearly insensitive to crystal size and $\tau_{0.6}$. Moreover, at high $\tau_{0.6}$ values the cirrus layer gives a very small contribution to the total signal. The channel is therefore not suitable to distinguish a plume feature from a surrounding cirrus anvil. The reflectances at 1.6 μm show instead a more pronounced sensitivity to the crystal size and $\tau_{0.6}$ due to the dependence of the single-scattering albedo on the particle size: small crystals scatter more incident radiation than the large ones.

Fig. 5 shows the simulated reflectances in the 3.9 μm channel as a function of $\tau_{0.6}$ of the cirrus layer and for small and large ice crystals. A much higher sensitivity to the crystal sizes is evident with respect to the 0.8 μm channel. In particular, small crystals induce higher reflectance values, while large ones show lower

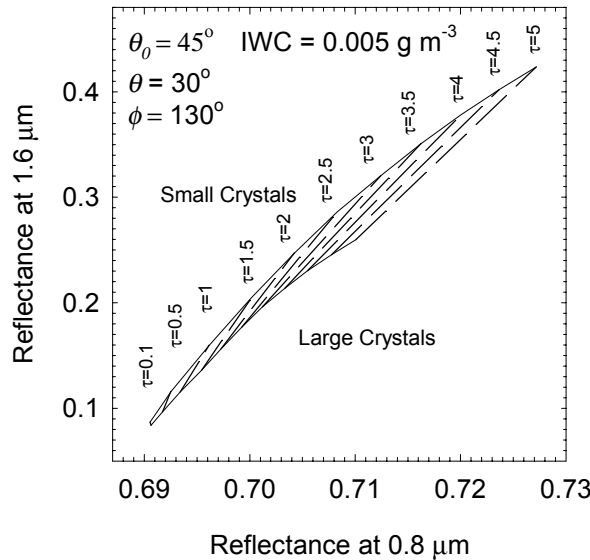


Figure 4. Simulated reflectance at 1.6 μm as a function of the reflectance at 0.8 μm . Solid curves refer to the two crystal size ranges and dashed lines are curves of constant $\tau_{0.6}$ of the cirrus layer.

reflectance values, almost constant with $\tau_{0.6}$. The cloud structure behaves very closely to a blackbody. Such a fact is essentially due to the dependence of the ice particle optical properties on particle size, as it can be seen from Fig. 2. These results seem to confirm that the enhanced reflectivity observed in the AVHRR channel 3 is due to cirriform layers composed of small ice crystals (whose dimensions are $\approx 3\text{-}4 \mu\text{m}$) on top of deep convection.

Fig. 6 and 7 show the dependence of the brightness temperature at 10.8 and 12 μm on $\tau_{0.6}$ and crystal size. The brightness temperature differences (BTD) between 10.8 and 12 μm are plotted as a function of $\tau_{0.6}$ (Fig. 6) and of the brightness temperature at 12 μm (Fig. 7). BTD are not instrumental for distinguishing the ice particle size since the differences between small and large crystals are relatively small. This would confirm the observations of Levizzani and Setvák (1996) on the scarce response of AVHRR thermal channels to the presence of ice crystal plumes.

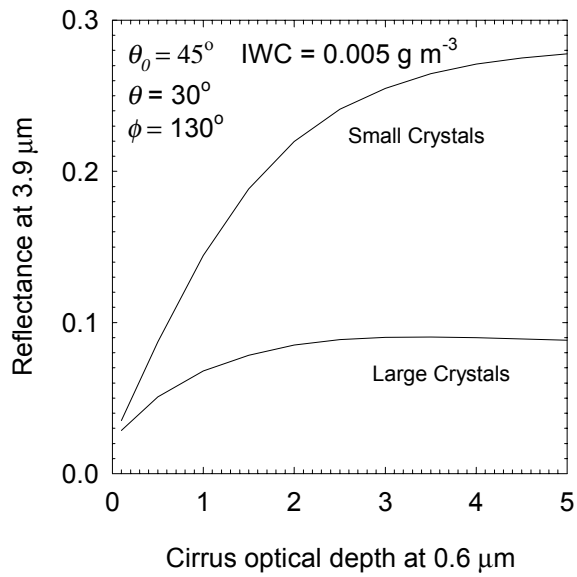


Figure 5. Reflectances at 3.9 μm as a function of the optical depth of the cirrus layer for the two ice crystal size ranges.

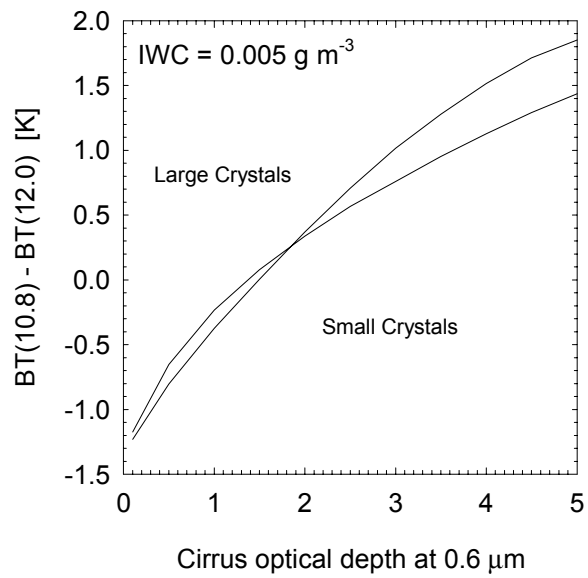


Figure 6. Brightness temperature differences between the channels at 10.8 and 12 μm as a function of the cirrus optical depth for small and large ice crystal ranges.

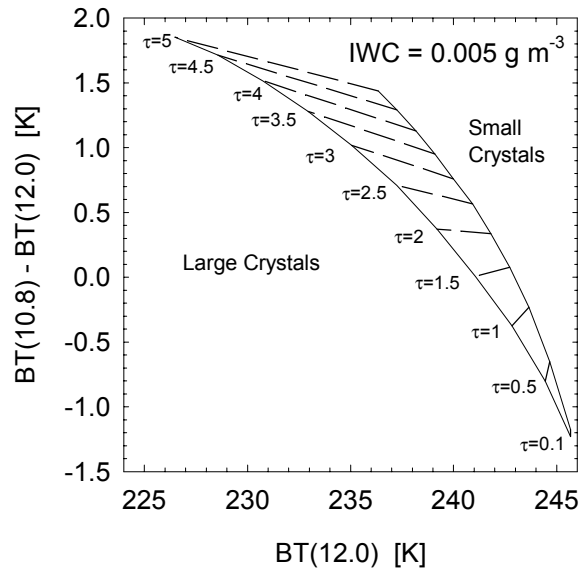


Figure 7. Brightness temperature differences between the channels at 10.8 and 12 μm as a function of the brightness temperature at 12 μm . Solid curves refer to the two ice crystal size ranges, and dashed lines are curves of constant $\tau_{0.6}$.

5. CONCLUSION

The present results point out that the MSG SEVIRI radiometer is effectively a good tool to study the cloud top of deep convective storms because of its spectral channels, spatial resolution and, in perspective, the short repeat cycle.

Encouraging results were obtained from the analysis of 3.9 μm reflectances in terms of detection and characterization of ice crystal plumes. The reflectances computed for the small crystals at 3.9 μm exhibit the same order of magnitude of those observed by Levizzani and Setvák (1996) in the AVHRR channel 3, seemingly confirming that very small ice crystals, whose size is 3-4 μm , compose cirriform layers on top of deep convection. On the other hand, plume features are nearly transparent at 0.8 μm . The thermal infrared channels at 10.8 and 12 μm do not show appreciable skills in detecting plume features as it was originally seen using AVHRR channel visual analysis. More research is on its way to implement a more realistic cloud structure. This initial sensitivity study will be followed by the use of a more complex model to account for the dynamics and a more detailed microphysics of the cloud scenario.

ACKNOWLEDGEMENTS

Work funded by: Agenzia Spaziale Italiana (ASI) through contracts *Studio del Ciclo Idrologico da Piattaforme Satellitari: Nubi e Precipitazioni* and *Sinergia GERB-SEVIRI nello Studio del Bilancio Radiativo a Scala Regionale e Locale*. EUMETSAT provided essential support through its visiting scientist program. Helpful discussions with S. A. Tjemkes and J. Schmetz are gratefully acknowledged.

REFERENCES

- Havemann, S., T. Rother, and K. Schmidt, 1998: Light scattering by hexagonal ice crystals. *Proc. Conference on light scattering by nonspherical particles: Theory, Measurements, and Applications*, 29 September-1 October, New York, 253-256.
- Key, J., 1998: STREAMER User's Guide. *Tech. Rep. 96-01*, Dept. of Geography, Boston Univ, 90 pp. (<http://stratus.ssec.wisc.edu/>).
- Key, J., and A. J. Schweiger, 1998: Tools for atmospheric radiative transfer: Streamer and FluxNet. *Computers & Geosciences*, **24**, 443-451.
- Levizzani, V., and M. Setvák, 1996: Multispectral, high-resolution satellite observations of plumes on top of convective storms. *J. Atmos. Sci.*, **53**, 361-369.
- Rother, T., 1998: Generalization of the separation of variables method for non-spherical scattering on dielectric objects. *J. Quant. Spectrosc. Radiat. Transfer*, **60**, 335-353.
- Rother, T., 1999: General aspects of solving Helmholtz's equation underlying eigenvalue and scattering problems in electromagnetic wave theory. *J. Electromagnet. Waves Appl.*, **13**, 867-888.
- Rother, T., and K. Schmidt, 1997: The discretized Mie-formalism for electromagnetic scattering. In *Progress in Electromagnetics Research (PIER)*, J. A. Jong Ed., EMW Publishing, Cambridge, MA, **17**, 91-183.
- Rother, T., S. Havemann, and K. Schmidt, 1999: Scattering of plane waves on finite cylinders with non-circular cross-sections. In *Progress in Electromagnetics Research (PIER)*, J. A. Jong Ed., EMW Publishing, Cambridge, MA, **17**, 79-105.
- Setvák, M., and C. A. Doswell, III, 1991: The AVHRR channel 3 cloud top reflectivity of convective storms. *Mon. Wea. Rev.*, **119**, 841-847.
- Stamnes, K., S. C. Tsay, and K. Jayaweera, 1988: Numerically stable algorithm for discrete-ordinate-method radiative transfer in multiple scattering and emitting layered media. *Appl. Opt.*, **27**, 2502-2509.